

# Transport Problems

Volume 16 Issue 2



## Problemy Transportu



GLIWICE 2021

SCIENTIFIC  
JOURNAL

**TRANSPORT PROBLEMS**

*Volume 16 Issue 2*

**PROBLEMY TRANSPORTU**

*Tom 16 Zeszyt 2*

QUARTERLY

WYDAWNICTWO POLITECHNIKI ŚLĄSKIEJ  
GLIWICE 2021

## CONTENTS

	Page
1. Konieczny J., Labisz K.: Materials used in the combat aviation construction .....	5
2. Ocieczek A., Mesinger D., Kaizer A. Zawadzki M.: The effects of particular factors connected with maritime transport on quality and safety of cereal as a cargo.....	19
3. Szczucka-Lasota B., Węgrzyn T., Szymczak T., Jurek A., Piwnik J., Wilczyński K.I.: Examination of mechanical properties of welds of Docol 1200M toward application in components of special vehicles .....	33
4. Hai D.T., Quyet N.X., Nguyen D.A.: Community participation for developing rural transport infrastructure in Dong Nai Province, Vietnam .....	45
5. Folęga P., Irlík M.: Effect of train position reporting on railway line capacity.....	59
6. Biliaiev M., Pshinko O., Rusakova T., Biliaieva V., Sładkowski A.: Computing model for simulation of the pollution dispersion near the road with solid barriers .....	73
7. Poliak M., Tomicová J., Jaśkiewicz M., Zhuravleva N., Fedorko G.: Neutralization of transport documents in road transport .....	87
8. Szpytko J., Salgado Duarte Y.: Robust simulation method of complex technical transport systems .....	101
9. Puzakov A.: Estimation of efficiency of electric power balance in automobiles .....	113
10. Vaičiūnas G., Steišūnas S.: Sperling's comfort index study in a passenger car with independently rotating wheels.....	121
11. Szymalski W.: Energy and CO <sub>2</sub> emission intensities of various modes of passenger transport in Warsaw .....	131
12. Pogorelov D., Rodikov A.: The trapezoidal finite element in absolute coordinates for dynamic modeling of automotive tire and air spring bellows. Part I: Equations of motion .....	141
13. Chislov O., Bogachev V., Zadorozhniy V., Kravets A., Bakalov M., Bogachev T.: Mathematical modeling of cargo flow distribution in a regional multimodal transportation system .....	153
14. Asenov A., Pencheva V., Ivanov B.: Methodology for expert evaluation of multimodal cargo transportation routes .....	167
15. Łukasik Z., Kozyra J., Kuśmińska-Fijałkowska A.: Reduction of CO <sub>2</sub> through application of a high-performance alternator.....	179
16. Tiutkin O., Neduzha L., Kalivoda J.: Finite-element analysis of strengthening the subgrade on the basis of boring and mixing technology.....	189
17. Raimbekov Z., Syzdykbayeva B.: Assessing the impact of transport and logistics on economic growth in emerging economies: a case study for the conditions of the republic of Kazakhstan.....	199
18. Ižvolt L., Dobeš P.: Evaluation of geotechnical tests (static load tests) on a selected optimised section of railway corridor no. Va.....	213

**Keywords:** automobile transport; pollution concentration; solid barriers

**Mykola BILIAIEV, Oleksandr PSHINKO**

Dnipro National University of Railway Transport named after academician V. Lazaryan  
Lazaryan, 2, Dnipro, 49010, Ukraine

**Tetiana RUSAKOVA\*, Viktoriia BILIAIEVA**

Oles Honchar Dnipro National University  
Haharin av., 72, Dnipro, 49010, Ukraine

**Aleksander ŚLADKOWSKI**

Silesian University of Technology  
Krasiński, 8, 40-019, Katowice, Poland

\*Corresponding author. E-mail: [rusakovati1977@gmail.com](mailto:rusakovati1977@gmail.com)

## COMPUTING MODEL FOR SIMULATION OF THE POLLUTION DISPERSION NEAR THE ROAD WITH SOLID BARRIERS

**Summary.** In this study, a numerical model is proposed for calculating pollution zones near the road, taking into account the geometry of the automobile transport, meteorological conditions, the location of the barriers and their height, and the chemical transformation of nitrogen oxides in the atmospheric air. The numerical solution is based on the integration of the mass transfer equations using the finite-difference method. To determine the components of the air flow velocity vector, a two-dimensional model of the potential flow is used, where the Laplace equation for the velocity potential is the modeling equation. Based on this numerical model, a software package has been developed that allows computational experiments and does not require large expenditures of computer time. Based on the results obtained, an assessment was made of the effectiveness of the use of barriers to reduce the level of air pollution near highways. It has been established that the use of barriers of different heights reduces the level of pollution behind the road by approximately 20-50%.

### 1. INTRODUCTION

Transport is one of the largest sources of pollution. For example, according to statistics for 2017 [1], about a quarter (23%) of greenhouse gas emissions in the EU were attributable to vehicle exposure. Despite the fact that thanks to very radical EU directives that plan to significantly reduce air emissions for all sectors of the European economy, the percentage ratio between individual sectors remains at the same level. As an example, the data obtained for the UK can be cited when this country was still in the EU [2]. The dynamics of nitrogen oxides emissions over an almost 30-year period is shown in Fig. 1a. A similar situation is observed in other European countries, for example, in Poland (Fig. 1b), although the decrease in emissions is not so noticeable here, which is explained by the relatively older car park. Despite the fact that there has been a significant reduction in this type of waste, road transport is the main source of these emissions.

The effect of harmful emissions on public health is one of the most significant problems of the modern industrial society. The given data on nitrogen oxides emissions were not chosen by chance, as this type of emissions is one of the most dangerous. The authors are not health professionals, so it is best to refer to works by well-known authors. In particular, an article [3] states: "Nitrogen oxide is a traffic-related pollutant, as it is emitted from automobile motor engines. It is an irritant of the respiratory system as it penetrates deep in the lung, inducing respiratory diseases, coughing, wheezing,

dyspnea, bronchospasm, and even pulmonary edema when inhaled at high levels”. It should be noted that nitrogen oxides are only one of the components of harmful emissions emitted by road transport. There are many more sources that analyze the harmful effects of emissions from road transport on human health.

Air pollution is one of the most serious environmental problems of all large urban centers. Emissions from automobile transport in large cities significantly increase the pollution rates of all environmental components. Dust and aerosol particles get deposited on the plants, absorbed by the upper layers of the soil, and washed out by precipitation and drainage flows. A large number of toxic substances that enter the atmospheric air are distributed at the level of the human respiratory system, causing various diseases. Harmful substances spread along both sides of the motorways, having a negative effect on drivers, pedestrians, and the population in general, whose places of residence are located near the roads. The composition and amount of exhaust gas emissions depend both on the condition of the engine and its technical level and on the type of fuel, but anyway, emissions contain a large number of toxic compounds, including benzopyrene, aldehydes, nitrogen oxides, sulfur dioxide, carbon, and lead.

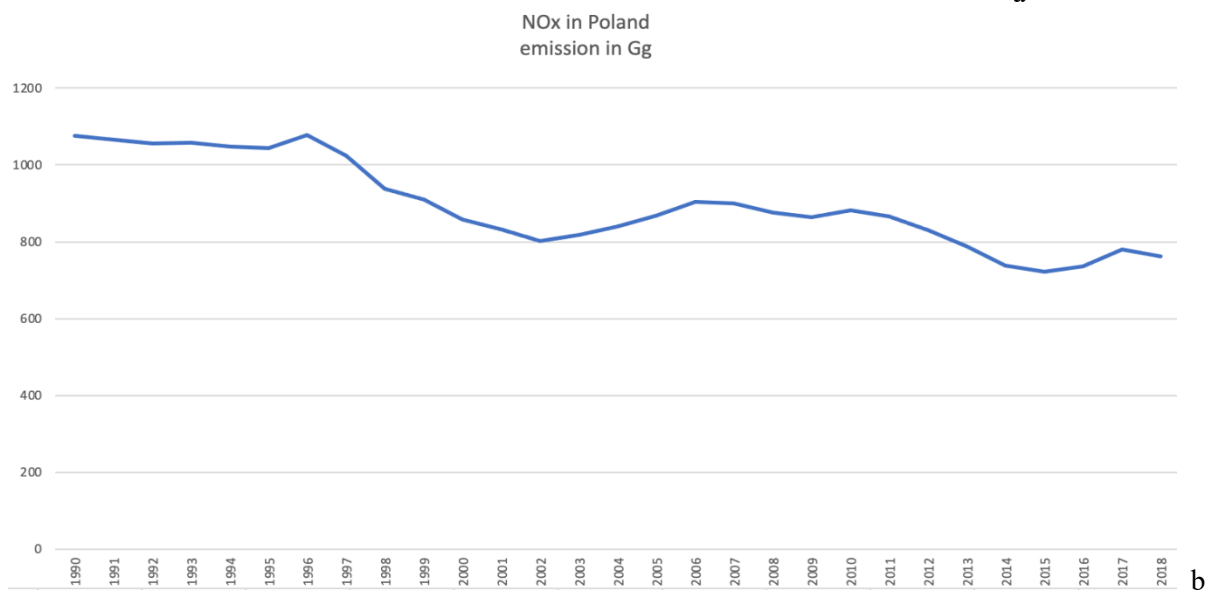
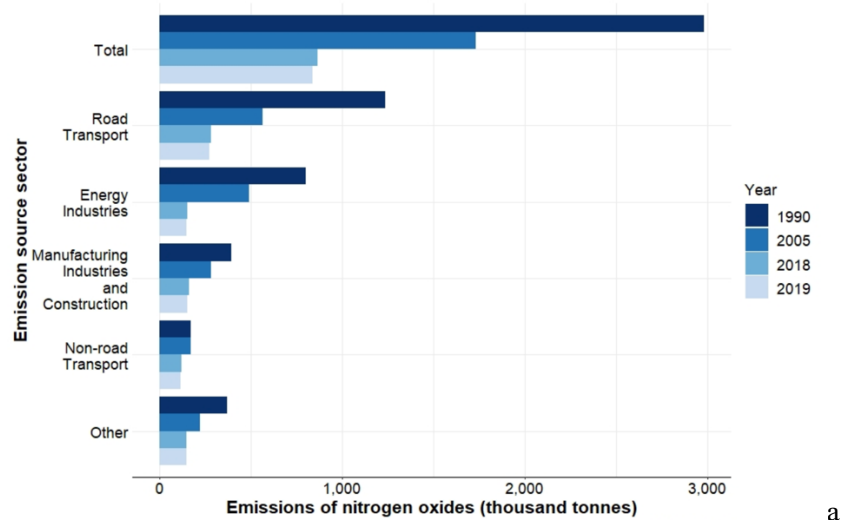


Fig. 1. Annual emissions of nitrogen oxides by 2019 major emissions sources: a) in UK 1990, 2005, 2018 and 2019 [2]; b) in Poland on the base of [19]

There are conflicting trends. On the one hand, new European emission standards are being introduced for road transport in Europe, for example, for passenger cars, the Euro 6d standard was

approved in January 2020. On the contrary, there is a constant increase in the number of vehicles, the construction of new roads, transport hubs, and parking lots, which together occupy a significant percentage of urban areas. After certain scientific studies, the formation of zones along the roads, where the concentration of exhaust gases exceeds the maximum permissible level, was revealed. The concentration of harmful impurities in the air along highways depends on the organization of traffic on the roads, the characteristics of the traffic flow, environmental parameters, the location of buildings, and the presence of green spaces. In places with low traffic capacity, near public transport stops, the concentration of pollutants reaches a maximum, and the organization of continuous movement of automobile transport leads to a decrease of pollutants from automobile transport.

An obvious solution to the problem of environmental pollution in the area of high-traffic roads (motorways and expressways) is to build them as far as possible from settlements. Unfortunately, it is not always possible to find such technical solutions. This is especially true for areas with a high density of urban development. The territories of southern Poland can be considered as an example. There are large urban agglomerations here, for example, the Upper Silesian Industrial Region or the Krakow Metropolitan Area. These territories occupy significant areas, and it is difficult to build the main road that would not cross urban areas. Fig. 2 shows the central part of Katowice, which is crossed by the European A4 motorway. As you can see from the given route, walking distance to the central square of the city is 1.5 km. It is known that the use of highway noise barriers is effective not only in terms of protecting the population from noise effect from heavy traffic on expressways but also in terms of reducing local pollution in areas adjacent to highways [4]. These solutions are effectively used for the already mentioned problematic sections of motorways that cross densely populated urban areas. Fig. 3 shows the use of highway noise barriers on the previously described section of the A4 motorway in Katowice. Depending on the surrounding area, one-sided or two-sided barriers are used to surround the carriageway.

Minimizing the level of chemical pollution near motorways is an extremely important task. One of the effective ways is the usage of barriers that allow changing the trajectory of pollution particles and reducing the local level of chemical pollution [5–7] and its concentration. A number of factors affect the efficiency of the barriers: meteorological conditions (wind speed and direction), the intensity of pollutants' emission, and the presence of local obstacles, i.e. when installing barriers, it is important to take into account the specific local conditions. Moreover, the result of using barriers in comparison with green spaces is observed from the moment they were installed, regardless of the period of the year. Predicting the level of concentration of harmful particles in the presence of barriers is a necessary component at the design stage of new roads or when reengineering existing ones, taking into account changes in the width of traffic way, which can lead to the formation of stagnant zones on the leeward side of barriers, as well as to justify changes in traffic.

In many scientific research studies, modified Gauss and CFD models are used to solve this problem. Thus, in a study [8], the authors proposed a three-dimensional computational hydrodynamic CFD model, which is based on the  $k$ - $\epsilon$  turbulence model, and made comparisons with experimental studies in a wind tunnel. It has been shown that the usage of barriers with a height of 3 m to 18 m near the road reduces the maximum value of the pollutant concentration by 15–61%. In the paper by Mao et al [9], experimental studies of the road dust concentration were carried out and numerical CFD modeling was developed taking into account the influence of the roadside protective strip of vegetation. Jason et al [10] proposed the CFD model CTAG, which implements a multiparametric methodology that takes into account the particle velocity, exhaust gas properties, and meteorological conditions, but this model still requires large computing resources. In other studies [11–12], models of air pollution dispersion in light wind, stable, and transient conditions are proposed; dispersion models are investigated; and the role of atmospheric stability, wind speed, and boundary layer height on the concentration change in the course of experimental studies is shown. However, the proposed models [10–12] do not take into account the presence of obstacles (barriers), which significantly affects the aerodynamics of the flow. Moreover, comparative studies of the stationary Gauss models AERMOD, CALINE 3 and 4, ADMS, and RLINE [13] were carried out, which give similar results under inversion conditions but mixed results under convection conditions. These models do not take into account the change in the flow rate with time and the change in meteorological conditions; however,

the importance of taking these parameters into account is shown in other research studies [8-12]. Therefore, the modified Gaussian models are convenient and quick to calculate, but cannot take into account the presence of obstacles, namely barriers. CFD models are based on solving the Navier-Stokes equations; they can calculate any configuration, and they are the most powerful modeling tool, but for the implementation of such developments, a significant amount of time is required to obtain a result, as the calculation time can be several days.

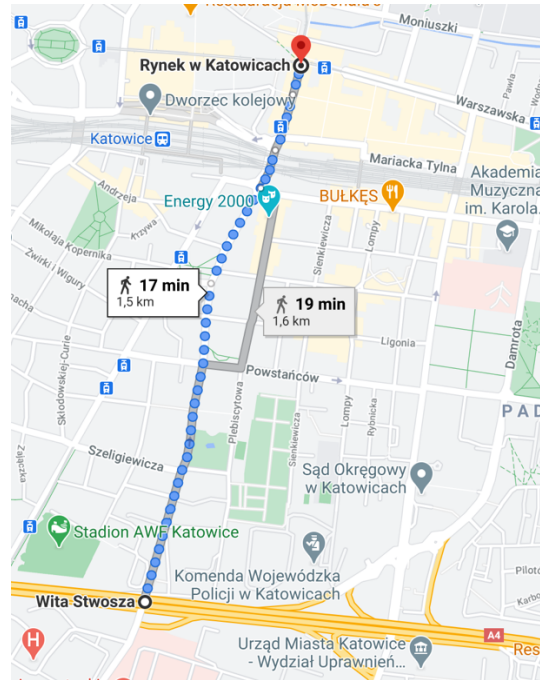


Fig. 2. Determining the distance for the central part of Katowice using Google Map



Fig. 3. Using highway noise barriers on the A4 motorway in Katowice

The purpose of this work is to develop an effective scientifically grounded model for calculating the level of atmospheric air pollution by automobile transport emissions, which allows to assess quickly the choice of barrier sizes and their location, but at the same time, it should be multifactorial and nonstationary.

## 2. STATEMENT OF THE RESEARCH PROBLEM

We consider a city road with continuous four-lane traffic; the width of one traffic lane is 3.75 m, and on one side of the road, it is supposed to place protective barriers, as there is a residential area (Fig. 4). The task is to calculate the zone of air pollution during the emission from automobile

transport ( $NO$ ,  $NO_2$ ), as well as to assess the effect of barriers of different heights on reducing the concentration of harmful substances behind the barrier.

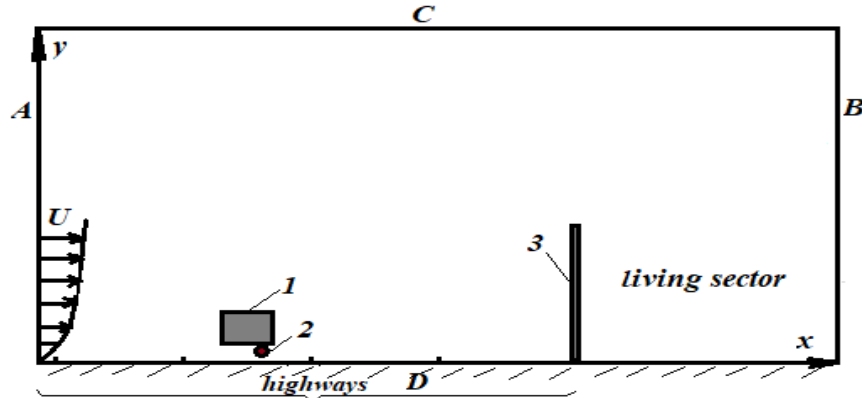


Fig. 4. Scheme of the calculated domain: 1 – automobile transport, 2 – emission source (exhaust pipe of a car), 3 – barrier; A, B, C, D – boundaries of the calculated domain

Under the action of sunlight ( $h_\nu$ ) nitrogen dioxide decomposes into nitric oxide and atomic oxygen, which converts oxygen ( $O_2$ ) into ozone  $O_3$ .

Accumulating in the lower layers of the atmosphere, these substances have a harmful effect on the human body. The main reactions in this case are reactions (1) – (3) [14-16]:



where  $J$  is the reaction rate parameter for the photolysis process depending on the amount of ultraviolet radiation, and  $k_1$  is the reaction rate parameter for  $NO$  [1/s].

In this paper, we consider the transformation process of nitrogen oxide and nitrogen dioxide near the road. The choice of only these pollutants is also due to the fact that to calculate the chemical transformation of emissions in the atmosphere, it is necessary to know the rates of their chemical reactions, which are determined experimentally and studied in other articles [14–16]. The solution of the task for forecasting air pollution by emissions from automobile transport is carried out into two stages.

Since the process of transformation of  $NO$ ,  $NO_2$ , and  $O_3$  in the atmospheric air is considered and it is taken into account that changes in the concentration of these substances are influenced by air flow rate, atmospheric diffusion, and emission intensity, the mass transfer equation is used for modeling [17]. This equation shows the change in concentration of  $NO$ ,  $NO_2$ , and  $O_3$  in the study area over time. Therefore, at the first stage of the solution, the process of transformation of these substances in the atmospheric air is modeled on the basis of mass transfer equations (4) - (6):

$$\begin{aligned} \frac{\partial C_{NO}}{\partial t} + \frac{\partial(uC_{NO})}{\partial x} + \frac{\partial(vC_{NO})}{\partial y} &= \frac{\partial}{\partial x} \left( \mu_x \frac{\partial C_{NO}}{\partial x} \right) + \frac{\partial}{\partial y} \left( \mu_y \frac{\partial C_{NO}}{\partial y} \right) + \\ &+ \sum_{i=1}^n Q_{NO_i}(t) \delta(x - x_{0i}, y - y_{0i}), \tag{4} \\ \frac{\partial C_{NO_2}}{\partial t} + \frac{\partial(uC_{NO_2})}{\partial x} + \frac{\partial(vC_{NO_2})}{\partial y} &= \frac{\partial}{\partial x} \left( \mu_x \frac{\partial C_{NO_2}}{\partial x} \right) + \frac{\partial}{\partial y} \left( \mu_y \frac{\partial C_{NO_2}}{\partial y} \right) + \end{aligned}$$



$$+ \sum_{i=1}^n Q_{NO_2 i}(t) \delta(x - x_{0i}, y - y_{0i}), \quad (5)$$

$$\frac{\partial C_{O_3}}{\partial t} + \frac{\partial u C_{O_3}}{\partial x} + \frac{\partial v C_{O_3}}{\partial y} = \frac{\partial}{\partial x} (\mu_x \frac{\partial C_{O_3}}{\partial x}) + \frac{\partial}{\partial y} (\mu_y \frac{\partial C_{O_3}}{\partial y}), \quad (6)$$

where  $C_{NO}(x, y, t)$ ,  $C_{NO_2}(x, y, t)$ , and  $C_{O_3}(x, y, t)$  – concentration of pollutants  $NO$ ,  $NO_2$ , and  $O_3$ , [kg/m<sup>3</sup>], respectively;  $Q_{NO_i}$  and  $Q_{NO_2_i}$  – emission intensity  $NO$  and  $NO_2$ , respectively, from the  $i$ -th source of emission (automobile transport), kg/(s·m<sup>3</sup>);  $u, v$  – wind speed vector components, [m/s];  $\mu = (\mu_x, \mu_y)$  – turbulent diffusion coefficient, [m<sup>2</sup>/s];  $x_{0i}, y_{0i}$  – coordinates of pollutant sources, [m]; and  $\delta(x - x_{0i}, y - y_{0i})$  – the Dirac delta function that simulates the presence of a pollutant release.

The diffusion coefficients are calculated by the formulas:  $\mu_x = k_0 \cdot U$ ,  $k_0 = (0,1 \div 1)$  m depending on the atmosphere stability level;  $U$  [m/s] – wind speed that is the known value of the wind flow velocity and can be calculated by the formula:  $U = U_1 \cdot (y / y_1)^{n_1}$ , where  $U_1$  is the value of the wind speed at a certain fixed height  $y_1 = 10$  m, and  $n_1 \approx 0.15 - 0.69$ , as it depends on the roughness of the underlying

surface and the stability class atmosphere ( $n_1 = 0.15$  was taken in the work); and  $\mu_y = k_1 \left( \frac{y}{y_1} \right)^m$ , where

$k_1 = (0,1 \div 0,2)$  m<sup>2</sup>/s within the surface layer of the atmosphere [17],  $m \approx 1$ . The degree of dependence for the velocity profile was taken for calculations according to the recommendations of prof. Berlyand M.E. and Byzova N.L. (Voeikov Main Geophysical Observatory), and the parameter  $n_1$  is taken from the works of prof. Bruyatskyi Ye.V. (Kyiv, Institute of Hydromechanics of NAS of Ukraine).

The delta function is zero everywhere, except for the cells where the  $i$ -th source of pollution is located. The emission of pollutants from automobile transport is modeled by point sources (cars) of a given intensity  $Q_{NO_i}, Q_{NO_2_i}$ , and  $n$  is the number of pollution sources.  $\sum_{i=1}^n Q_{NO_2 i}(t) \delta(x - x_{0i}, y - y_{0i})$

means that the action of all pollution sources with a specific intensity of the pollutant is taken into account, as well as the principle of superposition.

In discrete form, the Dirac delta function is «smeared» over the area (volume) of the difference cell while maintaining the total amount of pollution, i.e. the intensity of the source is considered as uniformly distributed over the cell; when the grid is refined, we arrive to the value at the point.

At the second stage of solving the task, the calculation of the chemical transformation of substances in the atmospheric air is carried out using the following dependences [14-15]:

$$\frac{dC_{NO}}{dt} = -k_1 \cdot C_{NO} \cdot C_{O_3} + J \cdot C_{NO_2}, \quad (7)$$

$$\frac{dC_{NO_2}}{dt} = k_1 \cdot C_{NO} \cdot C_{O_3} - J \cdot C_{NO_2}, \quad (8)$$

$$\frac{dC_{O_3}}{dt} = -k_1 \cdot C_{NO} \cdot C_{O_3} + J \cdot C_{NO_2}. \quad (9)$$

It is known that the emission  $NO_2$  is about 5% of the emission  $NO_x$ , and the rest 95%, is the emission  $NO$ . Chemical reactions and the photolysis reaction are interconnected in the atmosphere. The photolysis rate and the temperature-dependent reaction rate parameters are determined by expressions (10) – (11), obtained on the basis of processing the experimental results [15].

$$J = 8,14 \cdot 10^{-3} (0,97674 + 8,37 \cdot 10^{-4} \cdot (T - 273,15) + 4,5173 \cdot 10^6 \cdot (T - 273,15)^2), [s^{-1}] \quad (10)$$

$$k_1 = 44,05 \cdot 10^{-3} \exp\left(-\frac{1370}{T}\right), [ppb^{-1} s^{-1}]. \quad (11)$$

Nitrogen dioxide decomposes with the evolution of nitrogen oxide, and later nitrogen oxide is oxidized by ozone. After a series of successive reactions, one molecule of nitrogen oxide contributes to the destruction of 10 ozone molecules, because  $NO_2$  is more toxic than  $NO$ .

For numerous solutions of equations (7) - (9) taking into account dependencies (10) - (11), a program with the implementation of Euler method was developed [17].

This paper considers the dispersion of emissions from automobile transport for the case when protective barriers (barriers) are located near the road, as shown in Fig. 4. In this case, an uneven air flow velocity field will form in the study area. This field must be known to solve the modeling equations (4) - (6). A potential flow model is used to calculate the air flow under such conditions. In this case, the modeling equation is the Laplace equation for the velocity potential [17]:

$$\frac{\partial^2 P}{\partial x^2} + \frac{\partial^2 P}{\partial y^2} = 0, \quad (12)$$

where  $P(x,y)$  is velocity potential.

The corresponding boundary and initial conditions are set (Fig. 4):

- at the boundary  $A$  – the flow enters the computational domain, and the Neumann boundary condition  $\frac{\partial P}{\partial x} = U$  is set for the velocity potential;

- at the boundary  $B$  – the flow leaves the computational domain, and the Dirichlet boundary condition  $P = P_0 + const$  is set for the velocity potential, where  $P_0$  is a certain numerical constant equal to 100;

- at the boundary  $C$  – the upper boundary, a solid impenetrable wall, the non-penetration condition is set  $\frac{\partial P}{\partial y} = 0$ , as there cannot be an infinite boundary in numerical calculations, then it is chosen at a sufficient distance where the curvature of streamlines is insignificant;

- at the boundary  $D$  – the lower boundary, a solid impenetrable wall, the non-penetration condition  $\frac{\partial P}{\partial y} = 0$  is set;

- on all solid walls of barriers and the car, depending on the direction of the normal, the non-penetration condition must be satisfied.

The components of the air flow velocity vector are calculated based on the following dependencies [17]:

$$u = \frac{\partial P}{\partial x}, \quad v = \frac{\partial P}{\partial y}. \quad (13)$$

### 3. NUMERICAL MODELING

For the numerical integration of the Laplace equation (12), the method of conditional approximation is used. Firstly, the Laplace equation (12) is reduced to an evolutionary equation using the solution to be established in time [17]:

$$\frac{\partial P}{\partial \eta} = \frac{\partial^2 P}{\partial x^2} + \frac{\partial^2 P}{\partial y^2}, \quad (14)$$

where  $\eta$  is the fictitious time, at  $\eta \rightarrow \infty$ , the solution of equation (14) tends to the solution of the Laplace equation (12). Namely, stationary equation (12) is the limiting case of non-stationary equation (14), i.e. when the solution to equation (14) stops changing in time and enters a stationary regime, then this is the solution to equation (12). This approach was introduced by A.A. Samarsky and G.I. Marchuk when creating splitting methods. To solve this equation, it is necessary to set the initial condition, the potential field at  $\eta = 0$ . For example,  $P = 0$  can be taken in the entire computational domain at  $\eta = 0$ .

Difference approximation of the derivatives is used for numerical integration. A uniformly distributed rectangular grid in two-dimensional space is considered, each grid cell has  $\Delta x$ ,  $\Delta y$  dimensions along the corresponding Cartesian axis, and the coordinates of the grid nodes are calculated as follows:  $(x, y)_{i,j} = (i \cdot \Delta x, j \cdot \Delta y)$ ,  $i, j \in Z$ . Time is evenly sampled  $\eta = n \cdot \Delta \eta$ . The function  $P(x, y, \eta)$  is expressed at any node by a discrete analogue [17]:

$$P(x, y, \eta) = P(i \cdot \Delta x, j \cdot \Delta y, n \cdot \Delta \eta) = P_{i,j}^n. \quad (15)$$

To solve equation (14), the method of conditional approximation is used; in this case, the difference equations have the following form:

- at the first step of splitting

$$\frac{P_{i,j}^{n+\frac{1}{2}} - P_{i,j}^n}{\Delta \eta} = \left[ \frac{-P_{i,j}^{n+\frac{1}{2}} + P_{i-1,j}^{n+\frac{1}{2}}}{\Delta x^2} \right] + \left[ \frac{-P_{i,j}^{n+\frac{1}{2}} + P_{i,j-1}^{n+\frac{1}{2}}}{\Delta y^2} \right] \quad (16)$$

- at the second step of splitting

$$\frac{P_{i,j}^{n+1} - P_{i,j}^{n+\frac{1}{2}}}{\Delta \eta} = \left[ \frac{P_{i+1,j}^{n+1} - P_{i,j}^{n+1}}{\Delta x^2} \right] + \left[ \frac{P_{i,j+1}^{n+1} - P_{i,j}^{n+1}}{\Delta y^2} \right]. \quad (17)$$

Thus, when using the method of conditional approximation, the numerical solution of the two-dimensional equation (12) for determining the velocity potential is carried out in two steps: “16” and “17”. The first one contains the «intermediate» value of the potential  $P_{i,j}^{n+1/2}$  on the time layer « $n+1/2$ », and the second – the «final» value of the potential  $P_{i,j}^{n+1}$  on the time layer « $n+1$ ». The calculation ends when the condition  $|P_{i,j}^{n+1} - P_{i,j}^n| \leq \varepsilon$  is satisfied, where  $\varepsilon$  is the calculation accuracy,  $\varepsilon = 10^{-3} \div 10^{-6}$ , and  $n$  is the iteration number (the number of time steps).

The components of the velocity vector are calculated from the known values of the velocity potential:

$$u_{i,j} = \frac{P_{i,j} - P_{i-1,j}}{\Delta x}, \quad v_{i,j} = \frac{P_{i,j} - P_{i,j-1}}{\Delta y}. \quad (18)$$

To describe the numerical method for solving the transformation equations (4) – (6), we write them in the form of the generalized equation of convective-diffusion dispersion of an impurity:

$$\frac{\partial S}{\partial t} + \frac{\partial uS}{\partial x} + \frac{\partial vS}{\partial y} = \frac{\partial}{\partial x} \left( \mu_x \frac{\partial S}{\partial x} \right) + \frac{\partial}{\partial y} \left( \mu_y \frac{\partial S}{\partial y} \right) + \sum_{i=1}^n Q_{S_i}(t) \delta(x - x_i) \delta(y - y_i), \quad (19)$$

where  $S$  is the concentration of  $NO$ ,  $NO_2$ ,  $O_3$ ;  $u, v$  are components of the velocity vector;  $\mu = (\mu_x, \mu_y)$  is the coefficient of turbulent diffusion;  $Q_{S_i}$  is the emission intensity of  $NO$ ,  $NO_2$ ,  $O_3$ ;  $\delta(x - x_i) \delta(y - y_i)$  is Dirac delta function;  $(x_i, y_i)$  are coordinates of the emission source  $NO$ ,  $NO_2$  location; and  $t$  is time.

To solve equation (19), the following boundary conditions are set (Fig. 4):

- at the boundary  $A$  – the flow enters the computational domain, for the concentration of this impurity, a boundary condition  $S = S|_{\text{entrance}}$  is set that is the background concentration at time  $t=0$ , and in the absence of data, the concentration value is taken to be zero;

- at the boundary  $B$  – the flow leaves the computational domain; at the end of the computational domain in the numerical model, a boundary condition  $\frac{\partial S}{\partial x} = 0$  is fulfilled; and from a physical point

of view, this condition means that the diffusion process at the flow exit boundary is not taken into account;

- at the boundaries  $C, D$  and on all solid walls, depending on the direction of the normal, the non-penetration condition must be satisfied.

For the numerical integration of equation (19), it is split:

$$\frac{\partial S}{\partial t} + \frac{\partial uS}{\partial x} = \frac{\partial}{\partial x} \left( \mu_x \frac{\partial S}{\partial x} \right), \quad (20)$$

$$\frac{\partial S}{\partial t} + \frac{\partial vS}{\partial y} = \frac{\partial}{\partial y} \left( \mu_y \frac{\partial S}{\partial y} \right), \quad (21)$$

$$\frac{\partial S}{\partial t} = \sum_{i=1}^n Q_{S_i}(t) \delta(x - x_i) \delta(y - y_i), \quad (22)$$

In order to solve numerically equation (20), the following two-step splitting scheme is used:

- at the first step, the dependency is used

$$S_{i,j}^{n+\frac{1}{2}} = S_{i,j}^n - \Delta t \frac{u_{i+1,j}^+ S_{i,j}^{n+\frac{1}{2}} - u_{i,j}^+ S_{i-1,j}^{n+\frac{1}{2}}}{\Delta x} + \Delta t \mu_x \frac{-S_{i,j}^{n+\frac{1}{2}} + S_{i-1,j}^{n+\frac{1}{2}}}{2\Delta x^2} + \Delta t \mu_x \frac{-S_{i,j}^n + S_{i+1,j}^n}{2\Delta x^2}, \quad (23)$$

- at the second step, the dependency is used

$$S_{i,j}^{n+1} = S_{i,j}^{n+\frac{1}{2}} - \Delta t \frac{u_{i+1,j}^- S_{i+1,j}^{n+1} - u_{i,j}^- S_{i,j}^{n+1}}{\Delta x} + \Delta t \mu_x \frac{-S_{i,j}^{n+\frac{1}{2}} + S_{i-1,j}^{n+\frac{1}{2}}}{2\Delta x^2} + \Delta t \mu_x \frac{-S_{i,j}^{n+1} + S_{i+1,j}^{n+1}}{2\Delta x^2}, \quad (24)$$

where  $u^+ = \frac{u + |u|}{2}$ ,  $u^- = \frac{u - |u|}{2}$ .

For the numerical solution of equation (21), the following two-step splitting scheme is used:

- at the first step the dependency is used

$$S_{i,j}^{n+\frac{1}{2}} = S_{i,j}^n - \Delta t \frac{v_{i,j+1}^+ S_{i,j}^{n+\frac{1}{2}} - v_{i,j}^+ S_{i,j-1}^{n+\frac{1}{2}}}{\Delta y} + \Delta t \mu_y \frac{-S_{i,j}^{n+\frac{1}{2}} + S_{i,j-1}^{n+\frac{1}{2}}}{2\Delta y^2} + \Delta t \mu_y \frac{-S_{i,j}^n + S_{i,j+1}^n}{2\Delta y^2}, \quad (25)$$

- at the second step the dependency is used

$$S_{i,j}^{n+1} = S_{i,j}^{n+\frac{1}{2}} - \Delta t \frac{v_{i,j+1}^- S_{i,j+1}^{n+1} - v_{i,j}^- S_{i,j}^{n+1}}{\Delta y} + \Delta t \mu_y \frac{-S_{i,j}^{n+\frac{1}{2}} + S_{i,j-1}^{n+\frac{1}{2}}}{2\Delta y^2} + \Delta t \mu_x \frac{-S_{i,j}^{n+1} + S_{i,j+1}^{n+1}}{2\Delta y^2}, \quad (26)$$

where  $v^+ = \frac{v + |v|}{2}$ ,  $v^- = \frac{v - |v|}{2}$ .

For the numerical integration of equation (22), Euler's method is used [18]. This method is also used for the numerical solution of equations (7 - 9).

#### 4. RESULTS OF COMPUTATIONAL EXPERIMENTS

The developed forecasting method was used to solve the problem of assessing the pollution level near the road in the presence of an emission source (automobile transport), with the presence of a barrier and in its absence. The program for numerical calculation «Barrier» was created.

Several scenarios for the location of automobile transport and barriers were considered. The calculations were carried out with the following data: air flow rate 5 m/s, average intensity of nitrogen oxide emission  $Q_{NO_x} = 4.8 \text{ g/(s} \cdot \text{m)}$ , the authors obtained these data by measuring nitrogen oxide emissions from Daewoo Lanos cars with a service life of 7-10 years,  $NO_2$  is about 5% of the emission, and  $NO$  – 95%, the geometric dimensions of the region are 25 m along the Ox axis and 12.5 m along the Oy axis, which is directed vertically upward. The coordinates of the  $NO$  and  $NO_2$  emissions source are the coordinates of the exhaust pipe. It is assumed that this is a point source of emission; therefore,

in the mathematical model, it is specified by the Dirac delta function  $\delta_{ij}$ , and in the numerical model, by the position of the difference cell in which the emission source is located, namely,  $Q_{numerical} = Q(t)_{source} / (\Delta x \Delta y)$ , where  $Q(t)_{source}$  is the real emission of  $NO$  and  $NO_2$  from the automobile transport and  $\Delta x \Delta y$  is the area of difference cell. The road is modeled as a set of point sources. As a two-dimensional model is used, the wind direction is chosen across the highway (along the  $Ox$  axis). A model task is solved, taking into account the action of the barrier, and cars with the dimensions of width – 1.7 m and height – 1.6 m were considered as automobile transport. However, the calculation program allows taking into account any size of automobile transport.

At the first stage of numerical studies, calculations were carried out with an operating source of emission (automobile transport) on the first and fourth lanes of the road, without the presence of a barrier (Fig. 5), with a barrier height of  $H=2.8$  m (Fig. 6) and a height of  $H=5$  m (Fig. 7).

Figs. 5–7 show the distribution of  $NO$  concentration as a percentage of the maximum concentration value, obtained for a specific calculation option. Comparison of Figs. 5–7 shows that when a barrier appears, a zone with a large concentration gradient near it from the side of the highway is formed. This is due to the fact that the presence of the barrier helps to slow down the air flow and turn it in the vertical direction. Analysis shows that a barrier with a height of  $H=2.8$  m allows reducing the  $NO$  concentration behind the barrier from 60–65% to 25–30%, and a barrier with a height of  $H=5$  m reduces the concentration value to 10–15%.

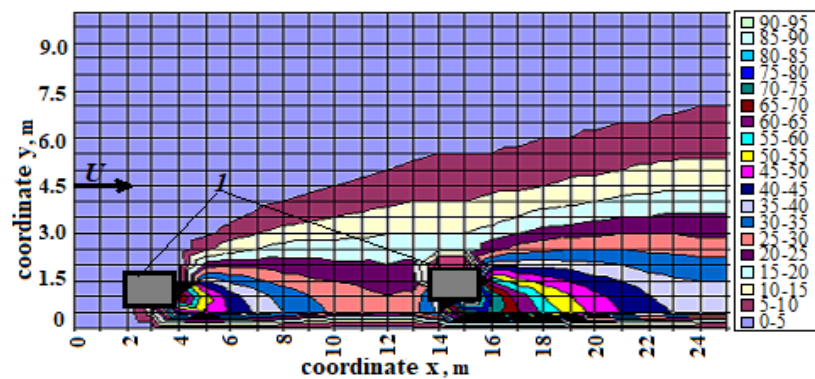


Fig. 5. Field of  $NO$  concentration in the absence of a barrier, where 1 – cars ( $C_{NO}$  as a percentage of  $(C_{NO})_{max} = 0.3887 \text{ mg/m}^3$ )

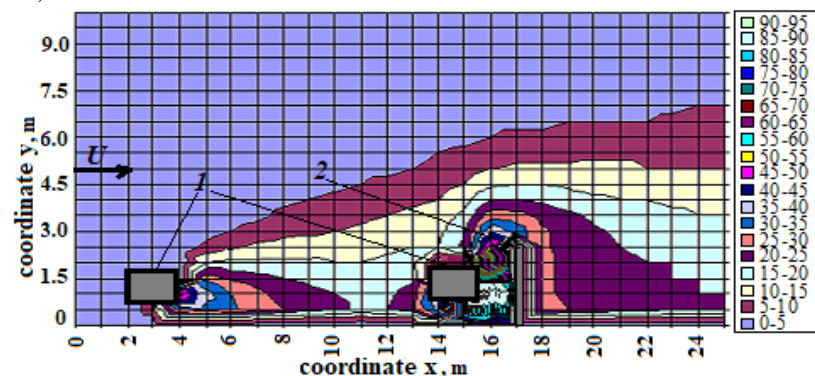


Fig. 6. Field of  $NO$  concentration with a barrier  $H = 2.8$  m: 1 – cars, 2 – barrier ( $C_{NO}$  as a percentage of  $(C_{NO})_{max} = 0.5554 \text{ mg/m}^3$ )

At the second stage of numerical studies, the concentration level behind the barrier was compared with a different number of emission sources on the road. Namely, the calculations were performed with the current emission source (automobile transport) only on the first lane of the road (Fig. 8), on the first and fourth lanes of the road (Fig. 7), on the first, second and fourth lanes of the road (Fig. 9) if barrier height of  $H=5$  m in each calculation option is used.

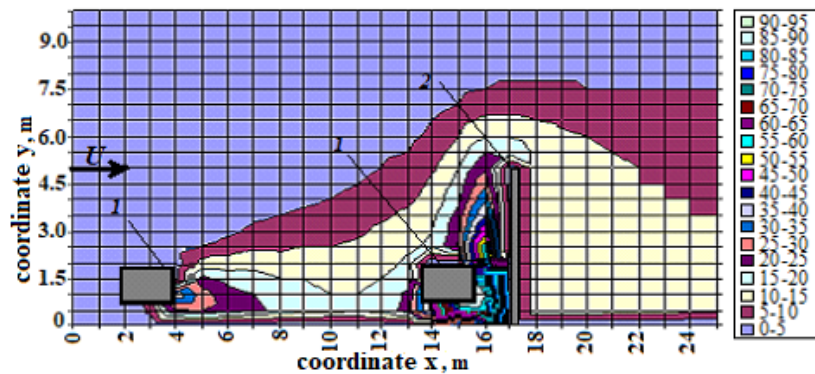


Fig. 7. Field of  $NO$  concentration with a barrier  $H=5$  m: 1 – cars, 2 – barrier ( $C_{NO}$  as a percentage of  $(C_{NO})_{max} = 0.7337 \text{ mg/m}^3$ )

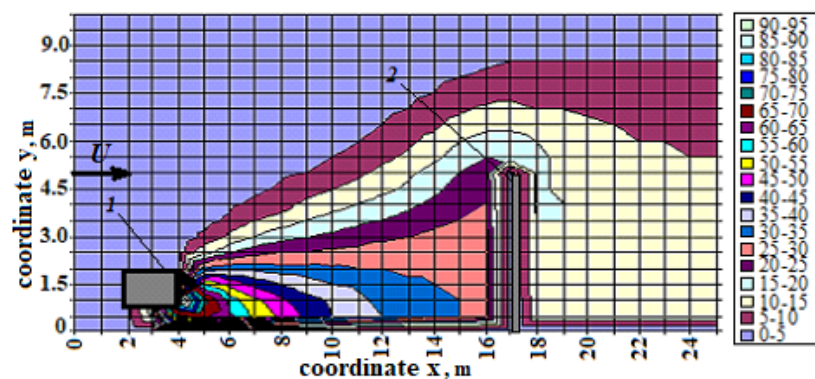


Fig. 8. Field of  $NO$  concentration in the presence of a barrier  $H=5$  m: 1 – car, 2 – barrier ( $C_{NO}$  as a percentage of  $(C_{NO})_{max} = 0.2864 \text{ mg/m}^3$ )

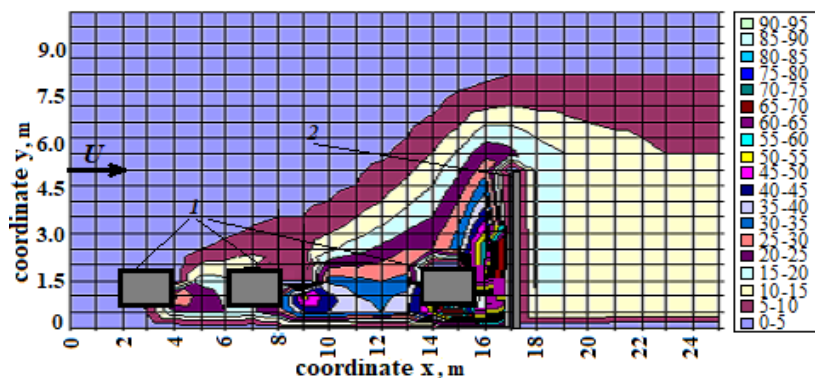


Fig. 9. Field of  $NO$  concentration in the presence of a barrier  $H=5$  m: 1 – cars, 2 – barrier ( $C_{NO}$  as a percentage of  $(C_{NO})_{max} = 0.92598 \text{ mg/m}^3$ )

Analysis of Figs. 7–9 shows the features of pollution zone formation. Figure 8 shows that the polluted zone, which is formed from the car in the direction of the barrier, namely in the section with the length along the  $Ox$  axis from 4 m to 15 m and the height along the  $Oy$  axis from 0 m to 2 m, practically corresponds to the zone of pollution. This zone of pollution is «classically» formed from a single point source. This is owing to the fact that the car body is located at a considerable distance from the barrier, which does not significantly affect the formation of the polluted zone. From the obtained concentration distribution, it can be seen that an increase in the number of emission sources on the road leads to an increase in the value of  $NO$  concentration behind the barrier from 10% to 15%, even in the presence of a barrier height  $H=5$  m.

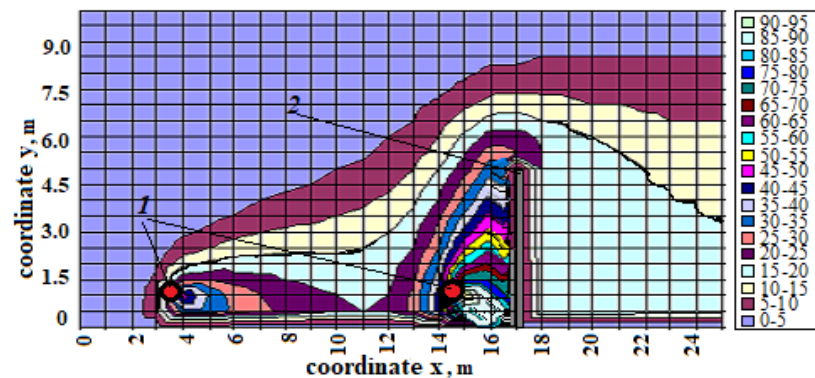


Fig. 10. Field of  $NO$  concentration in the presence of a barrier  $H = 5$  m: 1 – cars without taking in account geometry, 2 – barrier ( $C_{NO}$  as a percentage of  $(C_{NO})_{\max} = 0.4785 \text{ mg/m}^3$ )

If we consider two cars that have a body (Fig. 7), then the polluted zone is shorter. So, the zone with a pollution of 60–65% in Fig. 7 has a length up to 7.5 m along the  $Ox$  axis, whereas in Fig. 10, where the geometry of car body is not taken into account, this zone has a length of 11 m along the  $Ox$  axis. This is owing to the fact that in the absence of a car body, the polluted zone moves freely in the direction to the barrier, followed by its merging with the polluted zone from the car located closer to the barrier. Analyzing Fig. 7 and Fig. 10, it can be seen that the difference in the formation of the polluted zone is manifested in the section before the barrier, namely, the polluted zone with a concentration of 10–15% in Fig. 7 sags between two cars, whereas in Fig. 10, this fact is absent. This is due to the fact that two car bodies change the aerodynamics of the air flow; a «notch»-type area is formed, which leads to a change in the shape of the polluted zone on the highway. Comparison of the concentration distribution in Fig. 7 and Fig. 10 shows that not taking into account the geometry leads to overestimated concentration values by 25–30%, as the car is also an obstacle in the path of the moving stream, which significantly changes the air velocity field.

In the course of further research, calculations of pollutant concentration level were carried out taking into account changes in the geometry of the barrier. As you know, barriers are made not only vertical, i.e. perpendicular to the surface of the earth, but also of other forms, namely, different curvature of the profile and inclination relative to the ground, which significantly affects the resistance of the barriers to the incoming flow, and, accordingly, the appearance of stagnant zones on the windward side of the screens. In this paper, it is proposed to change the shape of the screen due to an additional horizontal component 1.25 m long at a height of 3.75 m from the earth's surface (Fig. 11–12), in order to show that the developed numerical model can take into account not only the geometry of cars but also the geometry of the screens. In Figs. 11 and 12, the shape of the polluted zone is practically the same up to the barrier in the direction of the air flow; however, behind the barrier, a significant difference in the shape of the polluted zone is visible, which is explained by the influence of the horizontal shelf on the aerodynamics of the air flow. The results of calculation show that the level of concentration behind the barrier at a height of the human respiratory system of 1.7 m is reduced to 10%. It is known that in the presence of obstacles in the computational domain, zones are formed where the streamlines have a large curvature. Under such conditions, some numerical models lose their stability, which limits their practical use, as in real conditions, there are a large number of combinations of the «road and barrier» location. The choice of such calculation scenarios shows that the constructed numerical model has a large margin of stability and can be used to calculate pollution zones in areas with different internal geometry.

The process of impurity propagation considered in this work is multifactorial, as it takes into account the mutual influence of emissions from several sources of pollution, the effect of the car body as a local obstacle, the location of barriers, the distance from the source to the barrier, and geometric form of the barrier. All these factors affect the formation of the impurity concentration field in the region under consideration.

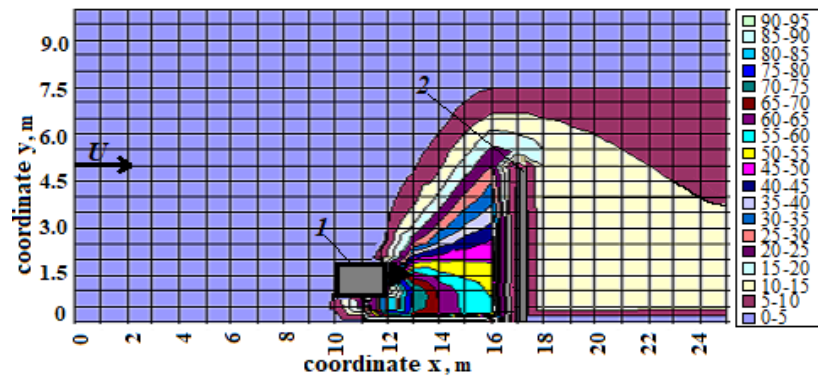


Fig. 11. Field of  $NO$  concentration in the presence of a vertical barrier  $H = 5$  m: 1 – car on the third lane, 2 – barrier ( $C_{NO}$  as a percentage of  $(C_{NO})_{\max} = 0.3742$  mg/m<sup>3</sup>)

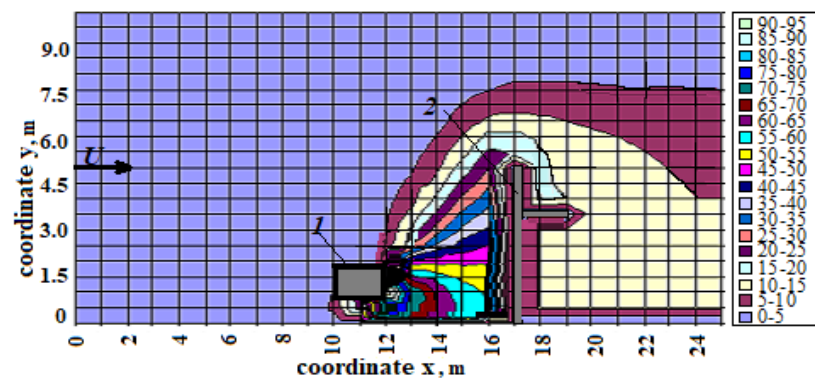


Fig. 12. Field of  $NO$  concentration in the presence of a vertical barrier  $H = 5$  m and a horizontal shelf: 1 – car in the third lane, 2 – barrier ( $C_{NO}$  as a percentage of  $(C_{NO})_{\max} = 0.3759$  mg/m<sup>3</sup>)

The constructed numerical model makes it possible to obtain pictures of chemical polluted zones and identify subzones where such contamination is more intense (Fig. 5–12). The identification of such sub-zones allows to recommend protective measures to minimize the level of contamination, for example, by changing the height of the barrier. From the obtained distribution of concentration field  $NO$  (Fig. 6–7), it can be seen that an increase in the height of the barriers leads to a decrease in the intensity of pollution in the area of the possible place of residence. Nevertheless, as can be seen from Fig. 7, an increase in the intensity of air pollution is observed in the area between the car in the fourth lane and the barrier. This is owing to the fact that the presence of the barrier leads to the formation of stagnant zones at its location on the side of the road, where the air flow rate is low. Thus, in these areas, there are locally high concentrations of chemical pollution, which requires the introduction of additional technical means to minimize the level of pollution in these stagnant zones (local suction).

## 5. CONCLUSIONS

A numerical model and software implementation for calculating pollution zones near the road are proposed. To describe the process of pollutant dispersion, we used mass transfer equations that take into account atmospheric diffusion and convective transport of impurities. The potential flow model was used to calculate the velocity field. The developed numerical model takes into account the chemical transformation of emissions  $NO$  и  $NO_2$  from automobile transport in the atmosphere. A feature of the developed model is the ability to carry out calculations taking into account the presence of barriers near the road of various heights and geometry, as well as taking into account the geometry of the car. The time for carrying out one computational experiment is 10 s. This model can be used in serial calculations for a preliminary assessment of air pollution near the road when designing protective barriers. On the basis of the computational experiments, the main regularities of the air flow behavior were established, and changes in the concentration of chemical pollution were shown depending on the presence of barriers with different heights and geometry, the position of the pollution



source and their amount, as well as on the geometry of the car. Further research is supposed to be carried out taking into account the terrain [18] and the joint use of barriers and other technical means (local suction) to reduce the level of chemical pollution of the air near the road.

## References

1. *How are emissions of greenhouse gases by the EU evolving?* Available at: <https://ec.europa.eu/eurostat/cache/infographs/energy/bloc-4a.html>.
2. *National Statistics. Emissions of air pollutants in the UK, 1970 to 2019 – Nitrogen oxides (NOx)*. Available at: <https://www.gov.uk/government/statistics/emissions-of-air-pollutants/annual-emissions-of-nitrogen-oxides-in-the-uk-1970-2018>.
3. Manisalidis, I. & Stavropoulou, E. & Stavropoulos, A. & Bezirtzoglou, E. Environmental and health impacts of air pollution: a review. *Frontiers in Public Health*. 2020. Vol. 8. No. 14. P. 1-13.
4. Baldauf, R. & Thoma, E. & Khlystov, A. & et al. Impacts of noise barriers on near-road air quality. *Atmospheric Environment*. 2008. Vol. 42. P. 7502-7507.
5. Bruno, L. & Fransos, D. & Lo Giudice, A. Solid barriers for windblown sand mitigation: Aerodynamic behavior and conceptual design guidelines. *Journal of Wind Engineering & Industrial Aerodynamics*. 2018. No. 173. P. 79-90.
6. Li, B. & Sherman, D.J. Aerodynamics and morphodynamics of sand fences: A review. *Aeolian Research*. 2015. No. 17. P. 33-48.
7. Wonsik, C. & Shishan, Hu & Meilu, He & Kozawa, K. *Spatial heterogeneity of roadway pollutant in Los Angeles*. Available at: [http://www.aqmd.gov/docs/defaultsource/technology\\_research/TechnologyForums/near-road-itigationmeasures/near\\_road\\_mitigation-agenda-presentations.pdf](http://www.aqmd.gov/docs/defaultsource/technology_research/TechnologyForums/near-road-itigationmeasures/near_road_mitigation-agenda-presentations.pdf).
8. Hagler Gayle, S.W. & et al. Model evaluation of roadside barrier impact on near-road air pollution. *Atmospheric Environment*. 2011. Vol. 45. No. 15. P. 2522-2530. DOI: <https://doi.org/10.1016/j.atmosenv.2011.02.030>.
9. Mao, Y. & Wilson, J.D. & Kort, J. Effects of a shelterbelt on road dust dispersion. *Atmospheric Environment*. 2013. Vol. 79. P. 590-598. DOI: <https://doi.org/10.1016/j.atmosenv.2013.07.015>.
10. Jason, Y. & et al. Modeling multi-scale aerosol dynamics and micro-environmental air quality near a large highway intersection using the CTAG model. *Science of the Total Environment*. 2013. Vol. 443. P. 375-386. Available at: <https://doi.org/10.1016/j.scitotenv.2012.10.102>.
11. Venkatram, A. & Snyder, M. & Isakov, V. Modeling the impact of roadway emissions in light wind, stable and transition conditions. *Transportation Research Part D: Transport and Environment*. 2013. Vol. 24. P. 110-119.
12. Venkatram, A. & Snyder, M. & Isakov, V. & Kimbrough, S. Impact of wind direction on near-road pollutant concentrations. *Atmospheric Environment*. 2013. Vol. 80. P. 248-258.
13. Heist, D. & et al. Estimating near-road pollutant dispersion: A model inter-comparison. *Transportation Research Part D: Transport and Environment*. 2013. Vol. 25. P. 93-105.
14. Overman, H.T. *Simulation model for NOx distribution in a street canyon with air purifying pavement*. Master thesis. University Twente, Netherlands. 2009. P. 1-99.
15. Merah, A. & Nouredine, A. modeling and analysis of NOx and O3 in a street canyon. *Der Pharma Chemica*. 2017. No. 9(19). P. 66-72.
16. Zhong, J. & Cai, X. & Bloss, W. Modelling the dispersion and transport of reactive pollutants in a deep urban street canyon. *Environmental Pollution*. 2015. Vol. 200. P. 42-52.
17. Biliaiev, M. & et al. Application of local exhaust systems to reduce pollution concentration near the road. *Transport Problems*. 2020. Vol. 15. No. 4. Part 1. P. 137-148. DOI: 10.21307/tp-2020-055.
18. Sang, J.J. A CFD study of roadside barrier impact on the dispersion of road air pollution. *Asian Journal of Atmospheric Environment*. 2015. Vol. 9-1. P. 22-30. DOI: <http://dx.doi.org/10.5572/ajae.2015.9.1.022>.
19. Officially reported emission data. *EMEP Centre on Emission Inventories and Projections*. Available at: <https://www.ceip.at/webdab-emission-database/reported-emissiondata>.